

Supplementary Materials: Prior-free Balanced Replay: Uncertainty-guided Reservoir Sampling for Long-Tailed Continual Learning

Anonymous Authors

1 APPENDIX

1.1 Dataset Details

Seq-CIFAR-10-LT and Seq-CIFAR-100-LT. The original versions of CIFAR-10 and CIFAR-100 contain 50,000 training and 10,000 testing images, respectively. Moreover, the class numbers are 10 and 100. Following [1], the long-tailed versions of them are sampled from the original ones with different imbalance ratios, mainly including 0.01, 0.02, 0.05, and 0.1. The testing set is unchanged. For the CL setting, the dataset is split into 5 tasks, each of which has 2 or 20 classes.

Seq-TinyImageNet-LT. The original versions of TinyImageNet contain 100,000 training and 10,000 testing images, respectively. The class number is 200. Following [1], the long-tailed version is sampled from the original ones with different imbalance ratios (IR), mainly including 0.01, 0.02, 0.05, and 0.1. The testing set is unchanged. For the CL setting, the dataset is split into 10 tasks, each of which has 20 classes.

1.2 Varying Imbalance Ratios

Different IRs on Seq-CIFAR10-LT and Seq-CIFAR100-LT under Ordered-LTCL. In this section, we provide the detailed experimental results under the ordered-LTCL setting on Seq-CIFAR10-LT and Seq-CIFAR100-LT with various IRs and buffer sizes. As shown in Table 2 and 3, our method outperforms previous methods by a large margin for both Class-IL and Task-IL settings. Particularly, with the different buffer sizes, the overall accuracy on the total classes is improved compared with the previous strong baselines DER and DER++. Additionally, it is observed that the methods resorting to gradients (GEM, A-GEM, GSS) seem to be less effective under this scenario, since the gradient information is influenced by imbalance distribution. In particular, compared to rehearsal methods, our method exhibits strong performance in most settings.

Different IRs on Seq-TinyImageNet-LT under Ordered-LTCL. Table 4 reports the detailed experimental results under the ordered-LTCL setting on the Seq-TinyImageNet-LT dataset with various IRs and buffer sizes. The observations are consistent with those on Seq-CIFAR10-LT and Seq-CIFAR100-LT datasets. Our method could achieve SOTA performance in almost all settings on such a large-scale dataset. We notice that a larger buffer size generally performs higher accuracy results but has a higher probability of influencing the learning of new tasks. Thus, we could conclude that boundary supporting samples carry more valuable information to prevent forgetting. Besides, the similarity and prototype information can be preserved in the memory.

Visualization of Selected Samples. Visualization can intuitively reflect the role of uncertainty-guided sampling for the memory buffer. During task evolution on the Seq-CIFAR-10-LT, we report the 2D t-SNE visualization of selected samples in memory

Algorithm 1 Reservoir Sampling with Uncertainty

```

Input: buffer  $\mathcal{M}$ , parameters  $\theta$ , number of seen samples  $N$ ,
        current data  $D_c$ 

 $\hat{D}_c[\cdot] \xleftarrow{MI} D_c, i = 0, N++$ 
for  $l = 0$  in range(length( $D_c$ )) do
    if  $|\mathcal{M}| > N$  then
         $\mathcal{M} \leftarrow \hat{D}_c[i++]$ 
    else
         $j = randomInteger(\min=0, \max=N)$ 
        if  $j < |\mathcal{M}|$  then
             $\mathcal{M} \leftarrow \hat{D}_c[i++]$ 
    return  $\mathcal{M}$ 

```

Algorithm 2 Balanced Experience Replay++

```

Input: dataset  $D$ , parameters  $\theta$ , learning rate  $\eta$ , scalar  $\tau_1$ ,  $\tau_2$ , and
        scalar  $\alpha$ 

 $\mathcal{M} \leftarrow \{\}$ 
while  $D$  not end do
    for  $(x, y)$  in  $\{D \cup \mathcal{M}\}$  do
         $\mathcal{L}_{kl} \leftarrow D_{KL}(f_{\theta^*}(x) \| f_{\theta}(x))$ 
         $\mathcal{L}_{t_c} \leftarrow MCE(f_{\theta}(x), y)$ 
         $\theta \leftarrow \theta + \eta \nabla_{\theta} (\mathcal{L}_{t_c} + \alpha \mathcal{L}_{kl})$ 
    return Updated  $\theta$ 

```

buffer for each task under the ordered-LTCL setting. As shown in Figure 3, different columns denotes the different tasks. Colorful points are associated with the samples that are selected into the memory buffer, while gray points are not. Guided by the uncertainty, most boundary supporting samples are stored in the memory buffer, which can reduce the influence of the forgetting problem. Due to class imbalance, new classes with fewer samples are influenced by both forgetting and majority classes, thus producing more uncertain samples for each task. Besides, with increasing buffer size, more boundary supporting samples of old classes can be stored, which can help to model task boundaries with new data.

REFERENCES

- [1] Bingyi Kang, Saining Xie, Marcus Rohrbach, Zhicheng Yan, Albert Gordo, Jiashi Feng, and Yannis Kalantidis. 2019. Decoupling Representation and Classifier for Long-Tailed Recognition. In *International Conference on Learning Representations*.
- [2] James Kirkpatrick, Razvan Pascanu, Neil Rabinowitz, Joel Veness, Guillaume Desjardins, Andrei A Rusu, Kieran Milan, John Quan, Tiago Ramalho, Agnieszka Grabska-Barwinska, et al. 2017. Overcoming catastrophic forgetting in neural networks. *Proceedings of the National Academy of Sciences* 114, 13 (2017), 3521–3526.
- [3] Zhihong Li and Derek Hoiem. 2017. Learning without forgetting. *IEEE Transactions on Pattern Analysis and Machine Intelligence* 40, 12 (2017), 2935–2947.
- [4] David Lopez-Paz and Marc'Aurelio Ranzato. 2017. Gradient episodic memory for continual learning. *Advances in Neural Information Processing Systems* 30 (2017), 115

Table 1: Detailed Dataset Information.

	Dataset	#Class	#Training	#Test	#Task
117	Seq-CIFAR-10-LT	10	$\leq 20,431$	10,000	5
118	Seq-CIFAR-100-LT	100	$\leq 19,573$	10,000	5
119	Seq-TinyImageNet-LT	200	$\leq 21,549$	10,000	10

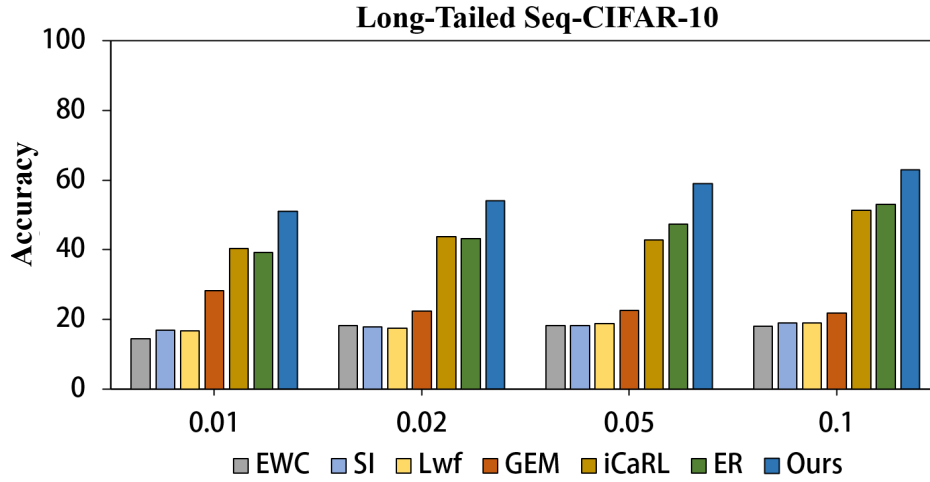


Figure 1: Performance comparisons of several classical CL methods (EWC [2], SI [8], Lwf [3], GEM [4], iCaRL [6], and ER [5, 7]) and the proposed PBR method. Existing method mainly focus on weight regularization or experience relay to alleviate the the catastrophic forgetting problem, which still suffer from the imbalance issue due to the deteriorated feature space. Our method can obtain higher recognition accuracy via learning an evolved feature space with prototype and boundary constraints.

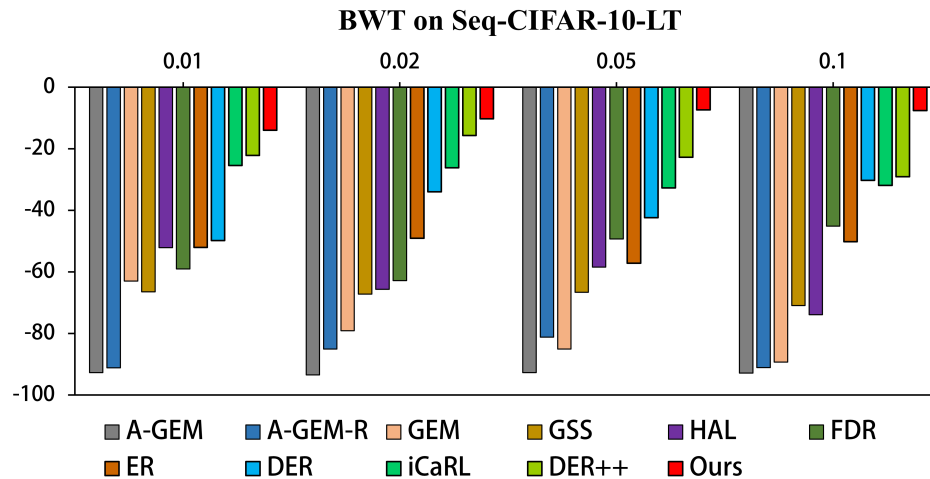


Figure 2: BWT results on Seq-CIFAR-10-LT under the ordered-LTCL setting. Buffer size is 200. Our method can achieve best results compared previous solutions.

- 6467–6476.
[5] Roger Ratcliff. 1990. Connectionist models of recognition memory: constraints imposed by learning and forgetting functions. *Psychological Review* 97, 2 (1990), 285.
[6] Sylvestre-Alvise Rebuffi, Alexander Kolesnikov, Georg Sperl, and Christoph H Lampert. 2017. icarl: Incremental classifier and representation learning. In *Proceedings*

- of the IEEE conference on Computer Vision and Pattern Recognition. 2001–2010.
[7] Matthew Riemer, Ignacio Cases, Robert Ajemian, Miao Liu, Irina Rish, Yuhai Tu, and Gerald Tesauro. 2018. Learning to Learn without Forgetting by Maximizing Transfer and Minimizing Interference. In *International Conference on Learning Representations*.

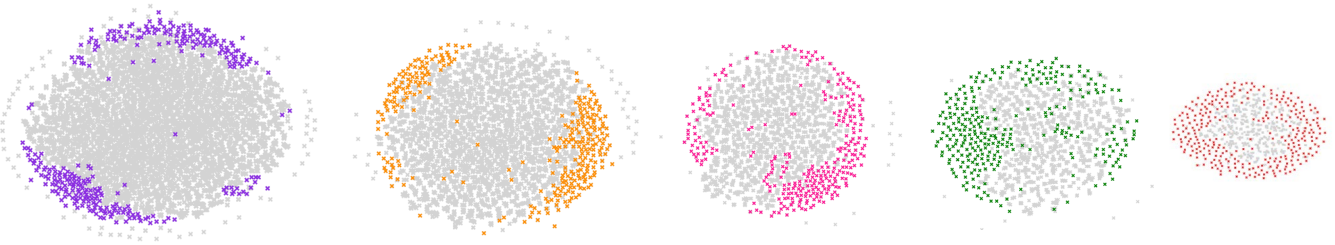
233
234
235
236
237
238
239
240
241
242243
244
245
246
247
248
249
250
251
252
253
254
255
256
257
258
259
260
261
262
263
264
265
266
267
268
269
270
271
272
273
274
275
276
277
278
279
280
281
282
283
284
285
286
287
288
289
290
291
292
293
294
295
296
297
298
299
300
301
302
303
304
305
306
307
308
309
310
311
312
313
314
315
316
317
318
319
320
321
322
323
324
325
326
327
328
329
330
331
332
333
334
335
336
337
338
339
340
341
342
343
344
345
346
347
348

Table 2: Ordered-LTCL Accuracy on Seq-CIFAR-10-LT. The architecture is ResNet18.

Buffer	Method	Seq-CIFAR-10-LT							
		0.01		0.02		0.05		0.1	
		Class-IL	Task-IL	Class-IL	Task-IL	Class-IL	Task-IL	Class-IL	Task-IL
-	oEWC	17.53±0.47	62.26±4.52	18.20±0.45	61.87±4.31	18.24±0.26	62.61±3.85	18.01±0.15	58.27±4.21
	SI	16.95±0.33	62.48±4.51	17.79±0.30	63.72±4.27	18.27±0.18	64.11±4.32	19.08±0.18	64.11±4.53
	LwF	16.70±0.20	59.44±1.32	17.56±0.18	27.45±1.33	18.85±0.12	61.39±1.25	18.97±0.01	33.93±1.17
	PNN	-	84.72±0.88	-	87.61±0.72	-	90.39±0.71	-	90.00±0.68
	ER	39.14±1.68	85.72±1.01	43.10±1.52	86.97±0.98	47.38±1.43	89.17±1.01	52.99±1.56	90.10±0.88
	GEM	29.20±0.97	82.83±0.87	22.40±0.89	86.60±0.97	22.52±1.12	86.22±1.24	21.91±0.87	89.35±0.98
	A-GEM	27.00±0.67	77.56±1.42	18.24±0.60	79.57±1.71	18.82±0.69	77.79±1.53	19.03±0.58	84.35±1.68
	A-GEM-R	17.86±0.87	71.44±1.64	17.24±0.71	76.80±1.32	18.14±1.02	75.49±1.68	18.13±0.61	73.29±1.59
	iCaRL	40.27±3.24	86.90±2.12	43.85±3.01	87.33±1.99	42.85±3.54	86.35±2.23	51.31±2.97	90.75±2.08
	FDR	28.54±3.17	72.52±0.99	31.13±2.36	85.67±1.02	43.06±1.98	90.17±0.88	40.78±2.68	88.53±0.97
200	GSS	35.71±3.64	85.74±1.87	36.85±3.67	87.07±2.03	38.90±3.54	86.76±1.67	37.40±3.76	88.46±1.94
	HAL	30.91±2.97	75.03±2.12	28.59±2.53	73.59±2.62	33.27±2.43	76.32±2.45	27.98±2.54	80.21±2.77
	DER	28.00±1.81	74.75±1.44	43.23±1.74	85.17±1.22	51.20±1.79	87.57±1.38	61.52±1.63	90.54±1.13
	DER++	37.65±1.87	83.25±1.24	44.03±1.75	87.35±1.11	55.63±1.66	89.64±1.17	60.68±1.48	90.98±0.95
	Ours	51.00±1.74	89.99±1.32	54.24±1.23	91.53±0.99	58.93±1.45	92.06±1.05	62.69±1.51	92.19±0.92
	ER	56.01±0.61	87.42±0.54	60.08±0.49	88.97±0.43	63.39±0.52	92.82±0.47	60.06±0.41	92.46±0.35
	GEM	28.46±1.77	84.16±0.75	22.41±1.45	89.05±0.66	20.57±1.32	90.83±0.67	27.65±1.13	90.01±0.56
	A-GEM	18.09±0.71	79.27±1.55	18.28±0.60	79.35±1.43	18.80±0.57	81.08±1.12	19.18±0.66	83.39±1.32
	A-GEM-R	11.32±0.67	57.97±1.54	17.54±0.63	78.14±1.54	18.05±0.62	74.95±1.52	20.75±0.67	79.06±1.32
	iCaRL	45.08±3.99	87.53±3.01	46.83±3.96	88.75±2.64	52.81±3.82	91.29±2.67	53.54±3.72	90.80±2.54
500	FDR	30.76±3.58	84.11±1.01	49.54±3.32	87.94±0.96	37.59±3.57	90.14±1.11	46.13±3.31	90.42±0.63
	GSS	47.63±4.15	87.65±1.32	42.21±4.33	87.60±1.64	44.60±4.03	90.19±1.42	49.93±4.56	91.54±1.57
	HAL	39.18±4.44	82.50±2.36	37.16±4.05	76.37±1.98	36.28±4.20	78.85±2.32	49.32±4.12	85.01±2.01
	DER	42.25±1.94	86.69±0.62	52.05±1.88	89.11±0.56	58.47±1.84	89.64±0.53	66.01±1.77	92.09±0.40
	DER++	48.68±1.88	88.42±0.64	44.30±1.68	88.50±0.61	61.46±1.74	91.23±0.53	67.22±1.63	92.21±0.41
	Ours	54.61±1.87	91.03±1.11	58.66±1.34	90.29±0.79	61.08±1.44	92.96±0.97	62.27±0.45	92.43±0.83

[8] Friedemann Zenke, Ben Poole, and Surya Ganguli. 2017. Continual learning through synaptic intelligence. In *International Conference on Machine Learning*. PMLR, 3987–3995.

Table 3: Ordered-LTCL Accuracy on Seq-CIFAR-100-LT. The architecture is ResNet18.

Buffer	Method	Seq-CIFAR-100-LT							
		0.01		0.02		0.05		0.1	
		Class-IL	Task-IL	Class-IL	Task-IL	Class-IL	Task-IL	Class-IL	Task-IL
-	oEWC	8.09±0.30	18.23±3.22	6.63±0.24	15.17±3.17	11.95±0.22	21.95±3.15	11.31±0.20	21.20±3.18
	SI	7.85±0.52	18.23±4.17	6.70±0.51	19.59±4.06	13.56±0.60	29.53±4.54	9.93±0.25	24.93±3.97
	LwF	8.47±0.20	14.80±2.13	8.29±0.21	15.22±2.20	13.52±0.17	19.51±2.10	13.66±0.10	20.37±2.04
	PNN	-	48.89±0.86	-	43.61±0.83	-	63.02±0.84	-	57.99±0.71
200	ER	14.72±2.31	42.32±1.17	16.54±2.11	46.81±1.14	19.21±2.34	53.03±1.27	19.57±1.94	55.73±1.07
	GEM	16.15±1.02	43.54±1.17	14.94±1.09	39.90±1.01	19.30±0.97	51.89±0.99	11.10±0.86	43.28±1.14
	A-GEM	11.91±0.45	30.57±1.57	7.88±0.57	26.48±1.62	13.15±0.38	37.08±1.49	8.12±0.40	29.81±1.49
	A-GEM-R	6.59±0.40	21.62±1.57	4.15±0.39	16.58±1.52	9.58±0.41	32.60±1.47	9.12±0.39	27.99±1.45
	iCaRL	22.85±3.54	49.62±2.21	20.40±3.43	46.17±2.27	30.33±3.56	54.83±2.39	26.67±3.47	54.55±2.21
	FDR	19.63±3.01	46.03±0.97	19.32±2.97	45.76±1.32	21.86±2.99	54.06±1.30	15.82±3.01	48.73±1.10
	GSS	11.78±4.12	40.56±1.57	14.15±4.52	43.45±1.68	15.30±3.97	45.61±1.27	16.34±3.87	47.20±1.09
	HAL	5.18±3.20	17.25±2.74	5.28±3.19	21.95±2.68	8.52±2.97	24.54±2.45	7.89±3.14	22.15±2.38
	DER	18.31±2.03	47.81±1.27	9.38±2.17	33.47±1.64	28.16±1.91	57.55±0.97	9.75±1.87	42.45±1.02
	DER++	19.62±1.95	46.22±1.14	7.75±1.99	31.81±1.43	26.45±1.74	56.70±1.03	11.28±1.79	46.23±0.93
500	Ours	24.18±1.67	50.66±0.85	20.65±1.87	47.53±0.92	31.32±1.58	54.99±0.98	28.69±1.67	55.19±1.13
	ER	20.50±0.36	49.63±0.31	25.05±0.38	54.87±0.32	25.28±0.33	58.02±0.29	27.33±0.31	61.23±0.36
	GEM	22.47±2.45	49.63±1.01	7.88±1.58	34.81±0.57	25.71±1.69	59.28±0.68	13.14±1.57	34.07±0.89
	A-GEM	8.68±2.57	49.63±2.23	7.77±1.78	28.22±0.73	12.96±1.77	34.82±0.93	13.78±1.86	34.00±1.01
	A-GEM-R	6.70±2.46	23.03±2.07	4.27±1.88	18.93±0.86	10.78±1.89	32.24±1.04	10.44±1.77	31.20±0.86
	iCaRL	24.51±2.03	50.74±1.08	24.3±1.81	50.40±0.97	33.61±1.73	60.94±0.92	30.80±1.60	58.97±0.89
	FDR	24.99±0.54	50.37±0.86	18.32±0.67	45.07±0.73	30.04±0.66	60.67±0.71	17.92±0.62	53.96±0.58
	GSS	14.74±3.97	44.82±0.95	16.22±3.86	45.29±1.00	18.55±3.74	52.66±0.91	19.09±3.60	55.26±0.88
	HAL	14.74±4.56	44.82±3.19	7.86±4.44	21.43±3.09	5.77±4.15	19.34±3.01	9.29±4.19	27.07±3.13
	DER	20.47±1.01	50.23±1.23	15.99±1.18	43.41±1.06	31.76±0.97	61.67±1.03	13.46±0.93	50.82±0.97
	DER++	20.90±0.98	51.88±1.14	15.80±1.05	43.55±0.94	30.69±1.06	62.66±1.11	17.43±0.93	53.89±1.02
381	Ours	25.05±1.32	52.23±1.29	25.48±1.17	50.85±1.09	34.33±1.25	63.86±1.27	32.40±1.20	60.59±1.11
	ER	20.50±0.36	49.63±0.31	25.05±0.38	54.87±0.32	25.28±0.33	58.02±0.29	27.33±0.31	61.23±0.36
	GEM	22.47±2.45	49.63±1.01	7.88±1.58	34.81±0.57	25.71±1.69	59.28±0.68	13.14±1.57	34.07±0.89
	A-GEM	8.68±2.57	49.63±2.23	7.77±1.78	28.22±0.73	12.96±1.77	34.82±0.93	13.78±1.86	34.00±1.01
	A-GEM-R	6.70±2.46	23.03±2.07	4.27±1.88	18.93±0.86	10.78±1.89	32.24±1.04	10.44±1.77	31.20±0.86
	iCaRL	24.51±2.03	50.74±1.08	24.3±1.81	50.40±0.97	33.61±1.73	60.94±0.92	30.80±1.60	58.97±0.89
	FDR	24.99±0.54	50.37±0.86	18.32±0.67	45.07±0.73	30.04±0.66	60.67±0.71	17.92±0.62	53.96±0.58
	GSS	14.74±3.97	44.82±0.95	16.22±3.86	45.29±1.00	18.55±3.74	52.66±0.91	19.09±3.60	55.26±0.88
	HAL	14.74±4.56	44.82±3.19	7.86±4.44	21.43±3.09	5.77±4.15	19.34±3.01	9.29±4.19	27.07±3.13
	DER	20.47±1.01	50.23±1.23	15.99±1.18	43.41±1.06	31.76±0.97	61.67±1.03	13.46±0.93	50.82±0.97
382	DER++	20.90±0.98	51.88±1.14	15.80±1.05	43.55±0.94	30.69±1.06	62.66±1.11	17.43±0.93	53.89±1.02
	ER	20.50±0.36	49.63±0.31	25.05±0.38	54.87±0.32	25.28±0.33	58.02±0.29	27.33±0.31	61.23±0.36
	GEM	22.47±2.45	49.63±1.01	7.88±1.58	34.81±0.57	25.71±1.69	59.28±0.68	13.14±1.57	34.07±0.89
	A-GEM	8.68±2.57	49.63±2.23	7.77±1.78	28.22±0.73	12.96±1.77	34.82±0.93	13.78±1.86	34.00±1.01
	A-GEM-R	6.70±2.46	23.03±2.07	4.27±1.88	18.93±0.86	10.78±1.89	32.24±1.04	10.44±1.77	31.20±0.86
	iCaRL	24.51±2.03	50.74±1.08	24.3±1.81	50.40±0.97	33.61±1.73	60.94±0.92	30.80±1.60	58.97±0.89
	FDR	24.99±0.54	50.37±0.86	18.32±0.67	45.07±0.73	30.04±0.66	60.67±0.71	17.92±0.62	53.96±0.58
	GSS	14.74±3.97	44.82±0.95	16.22±3.86	45.29±1.00	18.55±3.74	52.66±0.91	19.09±3.60	55.26±0.88
	HAL	14.74±4.56	44.82±3.19	7.86±4.44	21.43±3.09	5.77±4.15	19.34±3.01	9.29±4.19	27.07±3.13
	DER	20.47±1.01	50.23±1.23	15.99±1.18	43.41±1.06	31.76±0.97	61.67±1.03	13.46±0.93	50.82±0.97
383	DER++	20.90±0.98	51.88±1.14	15.80±1.05	43.55±0.94	30.69±1.06	62.66±1.11	17.43±0.93	53.89±1.02
	ER	20.50±0.36	49.63±0.31	25.05±0.38	54.87±0.32	25.28±0.33	58.02±0.29	27.33±0.31	61.23±0.36
	GEM	22.47±2.45	49.63±1.01	7.88±1.58	34.81±0.57	25.71±1.69	59.28±0.68	13.14±1.57	34.07±0.89
	A-GEM	8.68±2.57	49.63±2.23	7.77±1.78	28.22±0.73	12.96±1.77	34.82±0.93	13.78±1.86	34.00±1.01
	A-GEM-R	6.70±2.46	23.03±2.07	4.27±1.88	18.93±0.86	10.78±1.89	32.24±1.04	10.44±1.77	31.20±0.86
	iCaRL	24.51±2.03	50.74±1.08	24.3±1.81	50.40±0.97	33.61±1.73	60.94±0.92	30.80±1.60	58.97±0.89
	FDR	24.99±0.54	50.37±0.86	18.32±0.67	45.07±0.73	30.04±0.66	60.67±0.71	17.92±0.62	53.96±0.58
	GSS	14.74±3.97	44.82±0.95	16.22±3.86	45.29±1.00	18.55±3.74	52.66±0.91	19.09±3.60	55.26±0.88
	HAL	14.74±4.56	44.82±3.19	7.86±4.44	21.43±3.09	5.77±4.15	19.34±3.01	9.29±4.19	27.07±3.13
	DER	20.47±1.01	50.23±1.23	15.99±1.18	43.41±1.06	31.76±0.97	61.67±1.03	13.46±0.93	50.82±0.97
384	DER++	20.90±0.98	51.88±1.14	15.80±1.05	43.55±0.94	30.69±1.06	62.66±1.11	17.43±0.93	53.89±1.02
	ER	20.50±0.36	49.63±0.31	25.05±0.38	54.87±0.32	25.28±0.33	58.02±0.29	27.33±0.31	61.23±0.36
	GEM	22.47±2.45	49.63±1.01	7.88±1.58	34.81±0.57	25.71±1.69	59.28±0.68	13.14±1.57	34.07±0.89
	A-GEM	8.68±2.57	49.63±2.23	7.77±1.78	28.22±0.73	12.96±1.77	34.82±0.93	13.78±1.86	34.00±1.01
	A-GEM-R	6.70±2.46	23.03±2.07	4.27±1.88	18.93±0.86	10.78±1.89	32.24±1.04	10.44±1.77	31.20±0.86
	iCaRL	24.51±2.03	50.74±1.08	24.3±1.81	50.40±0.97	33.61±1.73	60.94±0.92	30.80±1.60	58.97±0.89
	FDR	24.99±0.54	50.37±0.86	18.32±0.67	45.07±0.73	30.04±0.66	60.67±0.71	17.92±0.62	53.96±0.58
	GSS	14.74±3.97	44.82±0.95	16.22±3.86	45.29±1.00	18.55±3.74	52.66±0.91	19.09±3.60	55.26±0.88
	HAL	14.74±4.56	44.82±3.19	7.86±4.44	21.43±3.09	5.77±4.15	19.34±3.01	9.29±4.19	27.07±3.13
	DER	20.47±1.01	50.23±1.23	15.99±1.18	43.41±1.06	31.76±0.97	61.67±1.03	13.46±0.93	50.82±0.97
385	DER++	20.90±0.98	51.88±1.14	15.80±1.05	43.55±0.94	30.69±1.06	62.66±1.11	17.43±0.93	53.89±1.02
	ER	20.50±0.36	49.63±0.31	25.05±0.38	54.87±0.32	25.28±0.33	58.02±0.29	27.33±0.31	61.23±0.36
	GEM	22.47±2.45	49.63±1.01	7.88±1.58	34.81±0.57	25.71±1.69	59.28±0.68	13.14±1.57	34.07±0.89
	A-GEM	8.68±2.57	49.63±2.23	7.77±1.78	28.22±0.73	12.96±1.77	34.82±0.93	13.78±1.86	34.00±1.01
	A-GEM-R	6.70±2.46	23.03±2.07	4.27±1.88	18.93±0.86	10.78±1.89	32.24±1.04	10.44±1.77	31.20±0.86
	iCaRL	24.51±2.03	50.74±1.08	24.3±1.81	50.40±0.97	33.61±1.73	60.94±0.92	30.80±1.60	58.97±0.89
	FDR	24.99±0.54	50.37±0.86	18.32±0.67	45.07±0.73	30.04±0.66	60.67±0.71	17.92±0.62	53.96±0.58
	GSS	14.74±3.97	44.82±0.95	16.22±3.86	45.29±1.00	18.55±3.74	52.66±0.91	19.09±3.60	55.26±0.88
	HAL	14.74±4.56	44.82±3.19	7.86±4.44	21.43±3.09	5.77±4.15	19.34±3.01	9.29±4.19	27.07±3.13
	DER	20.47±1.01	50.23±1.23	15.99±1.18	43.41±1.06	31.76±0.97	61.67±1.03	13.46±0.93	50.82±0.97
386	DER++	20.90±0.98	51.88±1.14	15.80±1.05	43.55±0.94	30.69±1.06	62.66±1.11</td		

Table 4: Ordered-LTCL Accuracy on Seq-TinyImageNet-LT. The model is ResNet18.

Buffer	Method	Seq-TinyImageNet-LT							
		0.01		0.02		0.05		0.1	
		Class-IL	Task-IL	Class-IL	Task-IL	Class-IL	Task-IL	Class-IL	Task-IL
50	ER	3.89±0.37	23.38±2.32	4.73±0.34	25.27±1.97	6.04±0.37	27.73±2.10	6.8±0.34	26.22±2.13
	A-GEM	2.99±0.14	11.12±0.20	3.27±0.11	11.56±0.18	5.12±0.08	14.57±0.14	6.32±0.06	18.17±0.07
	A-GEM-R	2.38±0.09	9.93±0.17	3.39±0.14	12.85±0.12	4.23±0.10	12.92±0.07	4.98±0.09	14.48±0.06
	FDR	3.86±0.23	21.13±0.77	4.57±0.20	20.86±0.75	5.77±0.43	24.05±0.88	6.49±0.71	26.79±0.74
	DER	4.52±0.78	23.75±0.76	5.01±0.68	23.81±0.78	6.36±0.69	24.83±0.80	6.41±0.62	24.68±0.77
	DER++	3.18±1.41	23.19±1.53	4.88±1.26	24.83±1.44	5.77±1.57	25.32±1.31	7.92±1.32	26.58±1.48
	Ours	4.83±1.67	23.80±1.55	5.49±1.54	25.07±1.63	6.78±1.34	26.08±1.23	8.32±1.45	29.98±1.52
200	ER	5.58±0.57	35.31±0.67	5.78±0.22	34.72±1.78	6.54±0.55	37.63±1.33	7.21±0.23	38.54±1.47
	A-GEM	3.34±0.24	12.16±0.21	2.75±0.25	10.95±0.17	5.06±0.23	15.22±0.20	6.17±0.14	17.52±0.10
	A-GEM-R	2.60±0.27	11.02±0.29	3.22±0.26	11.06±0.20	3.54±0.16	13.31±0.17	4.62±0.14	14.51±0.11
	iCaRL	7.01±0.62	29.13±1.68	8.18±0.55	33.49±1.54	8.36±0.60	34.05±1.65	10.39±0.57	36.88±1.53
	FDR	5.98±0.34	31.15±0.77	6.79±0.40	31.73±0.79	7.40±0.27	34.84±0.85	7.85±0.23	37.22±0.77
	DER	6.56±0.82	35.29±0.78	6.61±0.67	36.57±0.81	9.69±0.58	39.54±0.79	11.77±0.59	40.00±0.67
	DER++	6.92±1.53	34.52±1.36	8.00±1.45	35.48±1.33	8.75±1.14	37.20±1.32	10.61±0.97	39.96±1.01
	Ours	10.24±1.44	36.01±1.32	8.25±1.47	37.59±1.52	9.80±1.33	42.64±1.08	12.54±1.44	40.45±0.98
500	ER	8.49±0.59	39.61±0.94	9.23±0.60	41.42±0.89	8.88±0.56	42.36±0.66	9.61±0.54	44.91±0.75
	A-GEM	3.09±0.44	10.35±0.77	4.17±0.34	13.94±0.69	4.96±0.47	15.09±0.76	6.0±0.32	15.83±0.50
	A-GEM-R	2.42±0.43	11.11±0.78	3.04±0.37	11.09±0.62	4.53±0.38	13.25±0.74	5.07±0.42	14.51±0.61
	iCaRL	10.51±1.76	11.87±3.01	11.37±1.54	38.67±3.19	12.74±1.44	40.39±3.20	13.13±1.33	11.37±3.22
	FDR	10.21±0.45	39.42±1.03	10.76±0.37	43.22±1.00	10.46±0.35	45.16±1.14	10.00±0.33	45.86±0.86
	DER	9.22±1.23	43.38±1.08	9.71±1.39	44.59±0.97	11.28±1.15	45.83±1.04	13.70±1.15	49.11±0.98
	DER++	10.42±1.47	41.94±1.23	12.39±1.40	45.17±1.08	14.34±1.22	47.98±1.17	15.66±0.97	47.88±1.28
	Ours	10.78±1.25	44.13±1.36	13.12±1.34	46.54±1.17	16.33±1.18	49.24±1.17	16.34±1.07	50.43±1.29
1000	ER	12.81±0.43	46.99±0.35	13.17±0.47	49.06±0.33	13.44±0.39	52.06±0.36	13.38±0.37	53.25±0.31
	A-GEM	3.45±0.33	12.58±0.74	3.90±0.38	13.05±0.69	5.12±0.38	14.41±0.72	6.14±0.30	16.94±0.71
	A-GEM-R	2.47±0.37	10.44±0.64	2.68±0.37	12.54±0.74	4.46±0.31	13.04±0.77	4.78±0.29	14.12±0.64
	iCaRL	14.01±2.12	42.99±3.01	15.38±1.87	45.15±3.14	16.79±2.14	47.77±3.36	17.71±2.11	49.91±3.37
	FDR	16.77±0.67	47.01±0.79	16.49±0.77	49.29±0.84	15.74±0.71	50.74±0.83	16.36±0.56	54.05±0.69
	DER	8.81±1.01	43.53±1.23	9.44±0.97	41.19±1.10	13.02±0.90	49.92±1.04	17.53±0.79	55.44±0.94
	DER++	12.54±1.12	47.02±1.23	15.76±1.07	50.00±1.19	16.65±1.11	52.89±1.27	17.98±1.09	55.76±1.16
	Ours	12.97±1.32	50.13±1.17	16.92±1.22	51.00±1.21	17.33±1.17	55.44±1.20	18.45±1.10	58.55±1.16

501
502
503
504
505
506
507
508
509
510
511
512
513
514
515
516
517
518
519
520
521
522

559
560
561
562
563
564
565
566
567
568
569
570
571
572
573
574
575
576
577
578
579
580

Table 5: BWT results under ordered-LTCL.

Buffer	Method	Seq-CIFAR-10-LT			
		0.01	0.02	0.05	0.1
-	oEWC	-58.50	-58.33	-67.50	-70.82
	SI	-59.36	-53.78	-71.52	-71.03
	LwF	-58.93	-60.23	-68.93	-72.32
	PNN	-	-	-	-
200	ER	-52.28	-57.05	-61.71	-67.56
	GEM	-47.25	-41.58	-64.06	-73.13
	A-GEM	-57.80	-45.75	-72.16	-74.02
	A-GEM-R	-48.01	-48.06	-60.95	-62.99
	iCaRL	-21.91	-22.61	-24.14	-24.77
	FDR	-42.80	-45.87	-61.81	-67.93
	GSS	-56.68	-58.93	-66.27	-68.97
	HAL	-33.32	-40.08	-39.13	-41.21
	DER	-28.03	-40.67	-44.68	-66.50
	DER++	-35.93	-40.01	-49.57	-68.47
	Ours	-14.00	-10.30	-7.40	-7.58
	ER	-43.67	-46.81	-53.41	-56.65
	GEM	-36.18	-51.52	-56.08	-73.05
500	A-GEM	-60.53	-58.37	-70.98	-74.61
	A-GEM-R	-49.63	-46.85	-66.17	-65.11
	iCaRL	-18.42	-20.91	-19.53	-21.15
	FDR	-31.70	-42.18	-49.21	-62.52
	GSS	-50.77	-54.40	-62.19	-66.00
	HAL	-30.54	-34.88	-37.13	-41.21
	DER	-25.78	-32.83	-33.41	-56.67
	DER++	-24.00	-36.70	-35.10	-54.88
	Ours	1.70	-2.53	4.00	13.30

581

582

583

584

585

586

587

588

589

590

591

592

593

594

595

596

597

598

599

600

601

602

603

604

605

606

607

608

609

610

611

612

613

614

615

616

617

618

619

620

621

622

623

624

625

626

627

628

629

630

631

632

633

634

635

636

637

638

639

640

641

642

643

644

645

646

647

648

649

650

651

652

653

654

655

656

657

658

659

660

661

662

663

664

665

666

667

668

669

670

671

672

673

674

675

676

677

678

679

680

681

682

683

684

685

686

687

688

689

690

691

692

693

694

695

696